

Set-up of the standard 2D-DIC system for quantification of residual stresses

HAGARA Martin^{1,a}, PÁSTOR Miroslav^{1,b} and DELYOVÁ Ingrid^{1,c}

¹Department of Applied Mechanics and Mechanical Engineering, Faculty of Mechanical Engineering, Technical University of Košice, Letná 9; 042 00 Košice, Slovak Republic

^amartin.hagara@tuke.sk, ^bmiroslav.pastor@tuke.sk, ^cingrid.delyova@tuke.sk

Keywords: Digital Image Correlation, residual stress, full-field analysis, hole-drilling method

Abstract. The paper deals with the set-up of the standard single camera digital image correlation (DIC) system for the quantification of residual stresses. To find proper parameters of the camera some measurements were performed including founding for a convenient distance of the camera from analyzed specimen, creating of speckle-pattern with adequate speckle size and density, analysis of the calibration parameters influence on the measurement results obtained by camera calibration performed by calibration targets of various sizes. Moreover, the investigation of optimal correlation parameters used for evaluation of strains is present in the paper. Finally, the paper includes information about the results obtained by simulating the change of positions between the hole-drilling device and the camera during the incremental drilling process.

Introduction

Recently, non-contact optical methods are increasingly used to stress-strain analysis. It is caused by a fact that the full-field investigation provides a rich source of data in a relatively short time without the need for using any additional devices. Digital image correlation method can be considered as one of the youngest optical methods used in experimental mechanics because its development relates with the rapid development of computer vision noticed since the beginning of the nineties of the 20th century.

DIC is a full-field experimental method, based on the correlation of digital images, captured during the loading process of the analysed specimen. For the reason that the images are not correlated as wholes, but along small picture elements called facets, it is necessary to create a random black and white speckle-pattern on the specimen surface to make all its parts unique. There are two types of analysis performed by DIC systems:

- 2D analysis realised by a single camera system,
- 3D analysis realised by a system with minimally two cameras.

DIC method has been used in many modern, interesting fields of mechanical engineering e.g. biomechanics [1-3] or modal analysis [4-7], however, it can also be used in vibration [8-11], thermal or any other analysis [12-14].

The development in a field of DIC application for quantification of residual stresses has been noticed since 2005 when McGinnis et al. [15] performed the measurements using two different optical methods – photogrammetry and 3D-DIC – combined with the core-drilling method and obtained just a small error in normal stress. Since then, a lot of analysis has been carried out in the field of using DIC combined with a hole-drilling method to quantify residual stresses [16-18], leading to design special devices combining DIC with hole-drilling method [19-21].

In 2019 Hagara et al. [22] came with the idea to use standard (commonly delivered) 3D-DIC system Q-400 Dantec Dynamics combined with the standardized hole-drilling method. The uniform, residual stresses simulated in flat steel specimen, were calculated from strains obtained at three small areas, which locations corresponded to the measuring grids of strain gage rosette HBM 1-RY21-3/120 0°/45°/90°, due to a methodology given in standard ASTM E837-13a. The same procedure was realised on the opposite part of the specimen using the strain gage rosette. The relative difference between the simulated normal stress and normal stress quantified by DIC was ca. 3%, which can be considered as a sufficient correspondence.

However, the use of a standard 3D-DIC system for quantification of residual stresses has some drawbacks. The first one is that the cameras are not directed straightaway to the specimen, which causes a distortion of the images leading in many cases to correlation errors. The second one, a higher distance of the cameras from the analysed specimen, can cause problems with the correlation of the images. Then the higher facets have to be used, which leads to the loss of spatial resolution in the surrounding of the drilled hole edge. For these reasons, the author decided to realise some preparatory measurements to qualify the possibility of using their 2D-DIC Q-400 Dantec Dynamics system for quantification of residual stresses.

Preparatory measurements relating to the use of 2D-DIC system for quantification of residual stresses

To obtain the parameters needed for the realisation of 2D deformation analysis performed in the surrounding of the small hole the following experiment was realised. A specimen with 3.05 mm thickness, which shape and dimension are depicted in Fig. 1, was made from photoelastic material PSM-1 (Young's modulus of elasticity $E = 2500\text{MPa}$ and Poisson's ratio $\mu = 0.38$)

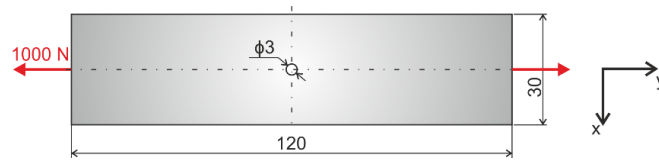


Fig. 1: Shape and dimensions of the analysed specimen

The reference image with a resolution of 2452x2056 px (the pixel density 111.45 px/mm) of the analysed part of the specimen can be seen in Fig. 2.

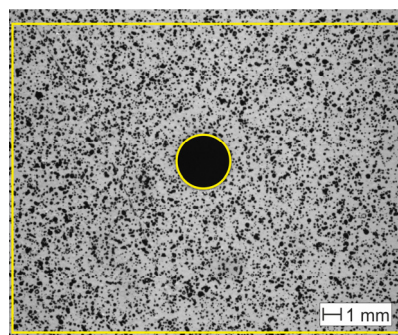


Fig. 3: Reference image of the specimen obtained by single camera DIC system and evaluation mask

In this case, a single-camera DIC system Q-400 Dantec Dynamics was arranged on a tripod in such a way, that the distance of its sensor to the specimen was approximately 130 mm (Fig. 3). Since the camera image plane is parallel to the object surface, distortion of the

image does not appear. This phenomenon is hard to overcome when using a multi-camera system.

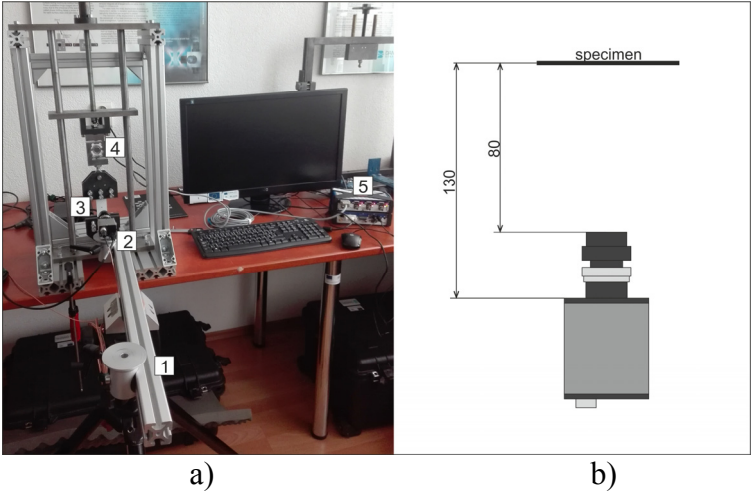


Fig. 2: a) The measurement chain: 1) tripod, 2) single CCD camera, 3) specimen, 4) force sensor, 5) HBM QuantumX CX22-W with amplifier QuantumX MX410-B, b) Proposed distance of the camera from the specimen

To situate the camera closer to the specimen was not possible, because in this case, the image of the specimen surface was not sharp enough. On the other hand, it was not suitable to increase the distance between the camera and the specimen, because the higher distance, the smaller pixel density, which could lead to the losing of important data.

The specimen was subsequently loaded by tension force acting in *y*-direction (see Fig. 1) until its magnitude reached 1000 N. Deformation of the specimen was measured by correlation system after each increase in the force of 100 N.

The calibration of the camera was realised using two calibration targets of different sizes – G1-01-WMB_9x9 with and G1-01_5-WMB_9x9 with 9x9 black and white fields of the particular fields’ size 1x1 mm and 1.5x1.5 mm. Comparison of their sizes with respect to the analysed field of view can be seen in Fig. 4.

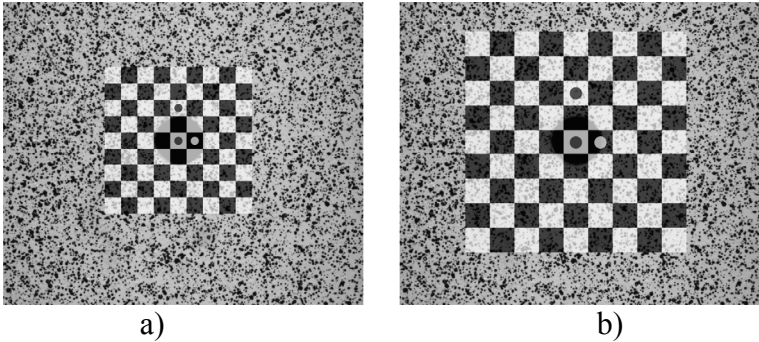


Fig. 4: Analyzed field of view in comparison with the size of calibration target: a) G1-01-WMB_9x9, b) G1-01_5-WMB_9x9

The calibration of the DIC system used for measurement is performed in such way that calibration target is captured in different positions and rotations until the information about the intrinsic and extrinsic parameters of the camera are not assessed. The manufacturer of the correlation systems states that for sufficiently accurate calibration just eight different positions of the calibration target are necessary. However, it was proven that the higher the number of different positions, the higher the accuracy of the measurement [23]. For that reason, twenty

different positions of the calibration targets were captured during both calibrations. The accuracy of the calibration is given by so-called calibration residuum. Approximately the same calibration residuum was achieved (0.276 px for the target with 1x1 mm fields and 0.283 px for the target with 1.5x1.5 mm) by both processes. Despite it, the obtained calibration parameters were not the same (see Fig. 5 and Fig. 6).

Intrinsic Parameters Camera Position 1 image:	
Focal length {x; y}:	{1e+004 ± 3e+002; 1e+004 ± 3e+002}
Principal point {x; y}:	{750 ± 130; 1230 ± 100}
Radial distortion {r ² ; r ⁴ }:	{-0,173 ± 0,011; 0,8 ± 0,3}
Tangential distortion {t ₁ ; t ₂ }:	{0,0025 ± 0,0009; -0,0039 ± 0,0011}
Extrinsic Parameters Camera Position 1 image:	
Rotation vector {x; y; z}:	{-3,105 ± 0,011; 0,004 ± 0,006; 0,06 ± 0,02}
Translation vector {x; y; z}:	{4,0 ± 1,1; -2,2 ± 0,9; 97 ± 2}
Calibration residuum:	0.276

Fig. 5: Calibration parameters assessed by the DIC system using calibration target GI-01-WMB_9x9

Intrinsic Parameters Camera Position 1 image:	
Focal length {x; y}:	{1e+004 ± 2e+002; 1e+004 ± 2e+002}
Principal point {x; y}:	{1090 ± 40; 550 ± 70}
Radial distortion {r ² ; r ⁴ }:	{-0,204 ± 0,013; 4,2 ± 0,8}
Tangential distortion {t ₁ ; t ₂ }:	{-0,0044 ± 0,0005; -0,0014 ± 0,0003}
Extrinsic Parameters Camera Position 1 image:	
Rotation vector {x; y; z}:	{3,116 ± 0,007; -0,057 ± 0,004; -0,015 ± 0,008}
Translation vector {x; y; z}:	{1,7 ± 0,3; 4,1 ± 0,6; 105,1 ± 1,4}
Calibration residuum:	0.283

Fig. 6: Calibration parameters assessed by the DIC system using calibration target GI-01_5-WMB_9x9

To investigate the influence of obtained calibration parameters on the results an analysis was realised. The aim of the analysis was to compare the results obtained experimentally with the results obtained numerically, whereby the data were compared just in three small areas, representing the measuring grids of the strain gage rosette HBM 1-RY21-3/120 0°/45°/90° used at the authors' workplace for quantification of residual stresses using the hole-drilling method. The numerical model was created in Ansys Workbench 17.0 in such way that mentioned areas, labeled in Fig. 7a as areas *a*, *b* and *c*, were uniformly divided and meshed by quadrilateral finite elements with the corresponding size. Subsequently, the numerical model was loaded by tension force 1000 N acting in *y*-direction (Fig. 7b).

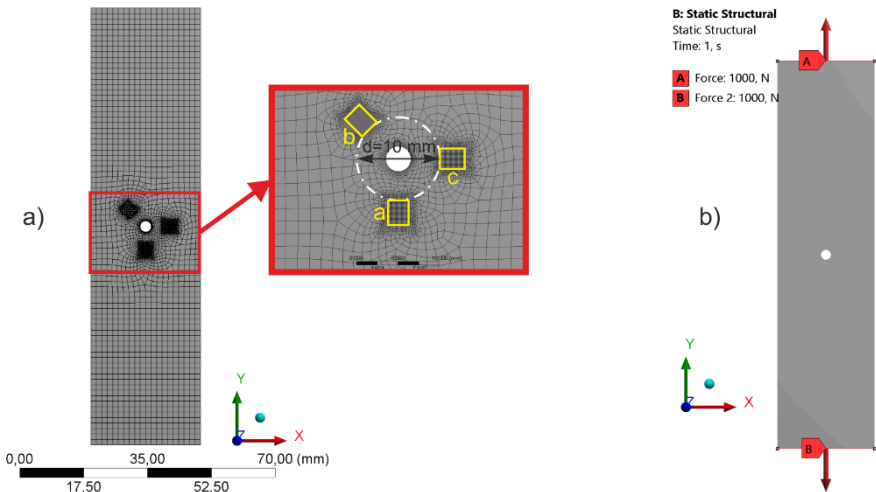


Fig. 7: Numerical model used for the comparison of the results with the results obtained experimentally

The mean values of equivalent von Mises stress calculated in areas a , b and c , were

$$\begin{aligned}\sigma_a^{Mises} &= 9.73\text{MPa}, \\ \sigma_b^{Mises} &= 12\text{MPa}, \\ \sigma_c^{Mises} &= 11.27\text{MPa}.\end{aligned}$$

In addition to the investigation of calibration parameters influence, the influence of the local regression smoothing level was analysed. The measurement was evaluated with different set facet sizes in the range from 15x15 px up to 30x30 px. Subsequently, the virtual gages in a form of polygons corresponding to the areas a , b and c were defined to calculate a parameter Δ_σ introduced by

$$\Delta_\sigma = \left(\frac{\text{mean}(\sigma_{i_{\text{exp}}}^{Mises})}{\text{mean}(\sigma_{i_{\text{num}}}^{Mises})} - 1 \right) \cdot 100 \quad (1)$$

where $\text{mean}(\sigma_{i_{\text{exp}}}^{Mises})$ are the mean values of equivalent von Mises stress obtained in areas a , b and c , by single camera DIC system and $\text{mean}(\sigma_{i_{\text{num}}}^{Mises})$ are the mean values of equivalent von Mises stress obtained in areas a , b and c by Ansys Workbench 17.0. Each smallest Δ_σ was then associated with the optimal setting of the kernel size with respect to the corresponding facet size.

The bar graphs in Fig. 8 and Fig. 9 depicts the dependence between the facet size and the optimal kernel size used in local regression smoothing. As can be seen, the obtained dependences are the same for both evaluations. In the bottom parts of Fig. 8 and Fig. 9, the dependences between the facet size and corresponding Δ_σ on analyzed areas a , b and c can be seen. While the differences obtained on area b , where Δ_σ reached ca. 14-16%, are quasi-same for both evaluations, the biggest difference between the obtained results appeared by comparing equivalent stresses on the areas a and c . For a reason that much smaller Δ_σ was obtained on the area a by using calibration parameters assessed by calibration performed with smaller calibration target, it seems to be more convenient to use calibration target G1-01-WMB_9x9 for the proposed arrangement of the 2D-DIC system.

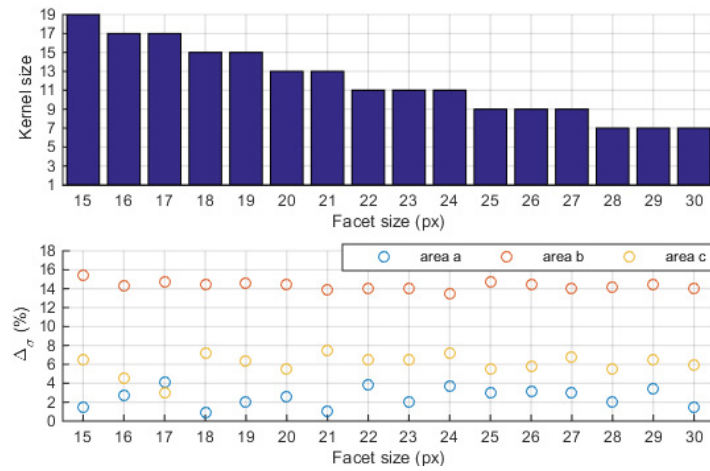


Fig. 8: Dependence between facet size and corresponding optimal kernel size used in local regression (upper graph), the dependence between the facet size and corresponding Δ_σ obtained on areas a , b and c (bottom graph) by evaluation using calibration parameters assessed by calibration with calibration target G1-01-WMB_9x9

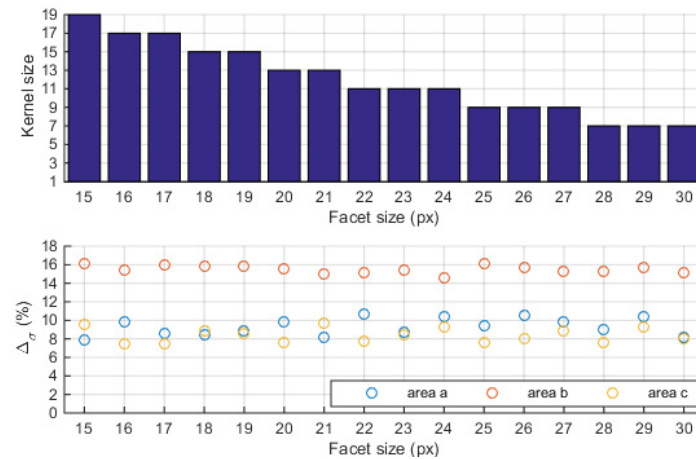


Fig. 9: Dependence between facet size and corresponding optimal kernel size used in local regression (upper graph), the dependence between the facet size and corresponding Δ_σ obtained on areas *a*, *b* and *c* (bottom graph) by evaluation using calibration parameters assessed by calibration with calibration target G1-01_5-WMB_9x9

In the last part of work, the authors dealt with the analysis of the influence of the camera position change, which can occur in case of incremental hole-drilling, because it is necessary to change position between the camera and the hole-drilling device after each step of drilling. For the analysis authors decided to use a function of the virtual bearing tool, which is a part of Dantec Dynamics control software Istra4D. The mentioned tool allows knowing the reference as well as the actual position of the camera (see Fig. 10). To obtain the mentioned influence, after the last step of loading (1000 N) the tripod with the camera was 10-times rotated clockwise around its vertical axis and subsequently (approximately) back to its previous position.

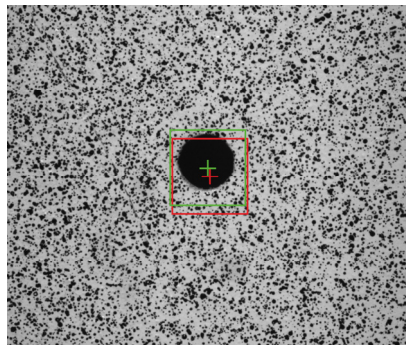


Fig. 10: Virtual bearing tool – reference position (red), actual position (green)

The evaluated strain fields corresponding to the last step of loading (1000 N) can be seen in Fig. 11. The facet size used for the correlation was set to 23x23 px, the level of local regression smoothing (Kernel size) was set to 11. The evaluation was performed using calibration parameters obtained with the smaller calibration target. As the data are obtained in the centres of facets, the diameter of the evaluated hole was approximately 3.5 mm, which still allows investigate the strains relatively near to the centre of the hole. By this phase of loading the strains on areas *a*, *b* and *c* reached the following mean values:

ε_a	ε_{b_x}	ε_{b_y}	$\varepsilon_{b_{xy}}$	ε_c
4.297e-3	-1.887e-3	5.617e-3	-0.128e-3	-1.512e-3

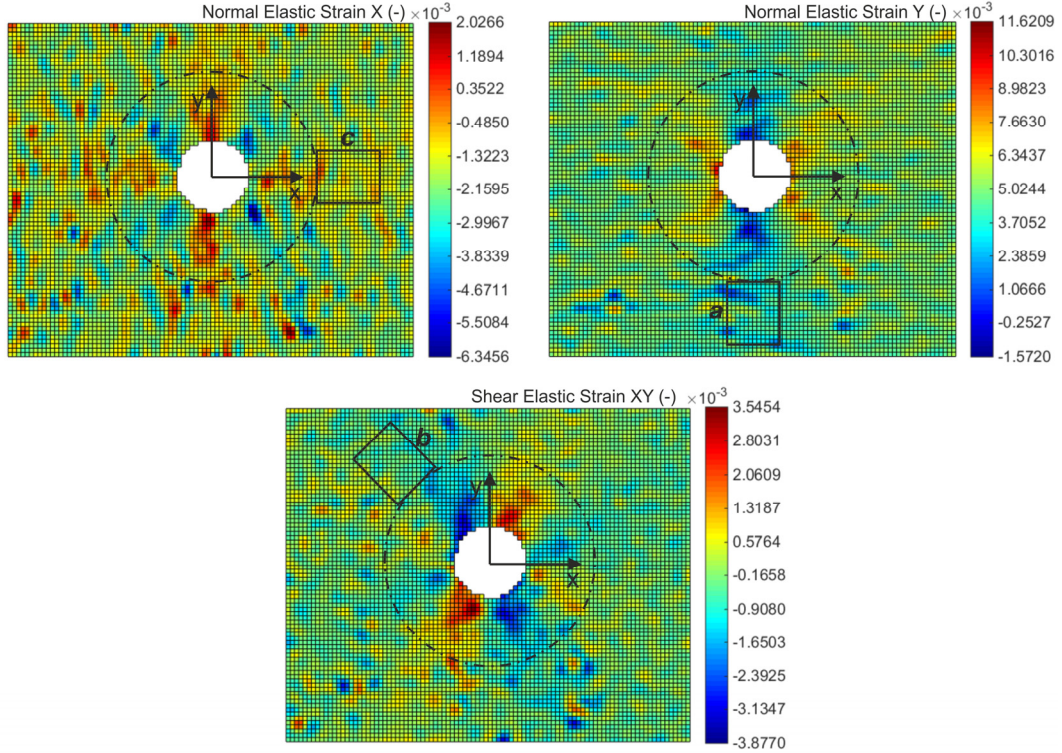


Fig. 11: Strain fields in the surrounding of the hole obtained by loading of 1000 N.

The relative differences in analysed quantities obtained after 10 rotations of the tripod with camera and its subsequent movement back to its previous position, by which the evaluated displacements do not exceed more than 0.06 mm, can be seen in Table 1.

Table 1: Relative difference in analysed quantities obtained after the camera's rotation and its subsequent movement back to its previous position

Reference values	Relative difference (%)									
	Rot. 1	Rot. 2	Rot. 3	Rot. 4	Rot. 5	Rot. 6	Rot. 7	Rot. 8	Rot. 9	Rot. 10
$\varepsilon_a = 4.297e-3$	-2.61	-7.29	2.26	7.12	5.27	4.39	-2.89	-4.64	6.27	6.16
$\varepsilon_{bx} = -1.887e-3$	-7.40	-18.39	-1.66	16.52	13.99	14.87	-9.12	-13.44	15.59	14.96
$\varepsilon_{by} = 5.617e-3$	-4.03	-3.73	1.41	5.71	7.61	3.15	-4.53	-4.11	4.89	6.12
$\varepsilon_{bxy} = -0.128e-3$	6.58	10.75	-19.17	-35.19	-18.59	-50.87	18.26	14.52	-31.01	-19.63
$\varepsilon_c = -1.512e-3$	-16.08	-22.94	5.99	30.63	17.68	31.92	-12.65	-20.25	25.78	18.52

Obtained differences could significantly influence the results of residual stress quantification. However, it has to be noted that the way of moving the camera back to its previous position was not very precise. For that reason, it will be a challenge for the authors to realise measurements and investigate, how the analysed data change if the displacement of the camera will be much smaller (e.g. in one order). For the realisation of such measurements, a unique automated hole-drilling device developed at the authors' workplace, allowing positioning in three mutually perpendicular directions with the accuracy of 1 μm , will be used. Recently, the device has been tested for the purposes of incremental hole-drilling combined with PhotoStress® method, however, it is assumed that it will be possible to use it also in combination with DIC system, attached on it.

Conclusions

The digital image correlation method allows a wide range of applications with high accuracy of the results. In the paper, some analyses lead to finding proper set-up of the 2D-DIC system combined with the hole-drilling method for the quantification of residual stresses, are described. Commonly used spray colours can be considered an effective way for creating random speckle-pattern with sufficiently small speckles and proper density. It seems that the results of stress/strain analysis depend markedly on the quality of camera calibration. For that reason, the authors propose to realise calibration of the camera more times to be sure that the calibration parameters are assessed correctly. The set of correlation parameters in a form of facet size and corresponding level of smoothing lead to the results, which do not differ markedly from the results obtained numerically. To ensure the accurate process of position changing between the camera and the hole-drilling device during incremental drilling can be considered as the biggest challenge. Moreover, in case if the released deformations are too small to be evaluated by DIC system with sufficient accuracy, the principle of the full-field measurement allows investigating displacements/strains with higher levels locating nearer to the centre of the hole. However, in this case, new calibration parameters used in the quantification process due to ASTM E837-13a will have to be found.

Acknowledgement

The paper is the result of projects implementation APVV 15-0435 and VEGA 1/0751/16.

References

- [1] M. Lezaja et al., Bond strength of restorative materials to hydroxyapatite inserts and dimensional changes of insert-containing restorations during polymerization, *Dental Materials* 31 (2015) 171-181.
- [2] V. Miletic et al., Local deformation fields and marginal integrity of sculptable bulk-fill, low-shrinkage and conventional composites, *Dental Materials* 32 (2016) 1441-1451.
- [3] K. Čolić et al., Experimental and numerical research of mechanical behaviour of titanium alloy hip implant, *Technički vjesnik* 24(3) (2017) 709-713.
- [4] R. Huňady, P. Pavelka, P. Lengvarský, Vibration and modal analysis of a rotating disc using high-speed 3D digital image correlation, *Mechanical Systems and Signal Processing* 121 (2019) 201-214.
- [5] A.J. Molina-Viedma et al. 3D mode shapes characterisation using phase-based motion magnification in large structures using stereoscopic DIC, *Mechanical Systems and Signal Processing* 108 (2018) 140-155.
- [6] A.J. Molina-Viedma et al. High frequency mode shapes characterisation using Digital Image Correlation and phase-based motion magnification, *Mechanical Systems and Signal Processing* 102 (2018) 245-261.
- [7] C.M. Sebastian, E., López-Alba and E.A. Patterson, A comparison methodology for measured and predicted displacement fields in modal analysis, *Journal of Sound and Vibration* 400 (2017) 354-368.
- [8] S. Barone et al., Low-frame-rate single camera system for 3D full-field high-frequency vibration measurements, *Mechanical Systems and Signal Processing* 123 (2019) 143–152.

- [9] M. Svoboda et al., Effect of Impacts on Human Head, *Manufacturing Technology* 15 (2) (2015) 226-231.
- [10] M. Svoboda et al. Force effect of strike and the possibility of causing a skull fracture of a human head, *Springer Proceedings in Mathematics and Statistics : 13th International Conference on Dynamical Systems : Łódź, 7-10 December, 2016*, 181 (2016) 353-360.
- [11] F. Klimenda et al. Investigation of Vertical Vibration of a Vehicle Model Driving Through a Horizontal Curve, *Manufacturing Technology* 15(2) (2015) 143-148.
- [12] M. Schrötter et al., Basic Thermal Field Analysis of a Small Turbo-Jet Engine, *Proceedings of NTAD 2018 - 13th International Scientific Conference – New Trends in Aviation Development*, (2018) 105-113.
- [13] R. Halama et al., Comparison of ESPI and DIC Strain Contours Measurements under Three Loading Cases, *Proceedings of Experimental Stress Analysis 2017 : 55th International Scientific Conference : Nový Smokovec, May 30-June 1, (2017)* 359-363.
- [14] Z. Paška et al. Strain Response Determination in Notched Specimens under Multiaxial Cyclic Loading by DICM, *Proceedings of Experimental Stress Analysis 2017 : 55th International Scientific Conference : Nový Smokovec, May 30-June 1, (2017)* 143-149.
- [15] M. J. McGinnis, S. Pessiki, H. Turker, Application of three-dimensional digital image correlation to the core-drilling method, *Experimental Mechanics* 45 (4) (2005) 359-367.
- [16] D. V. Nelson, A. Makino, T. Schmidt, Residual stress determination using hole drilling and 3D image correlation, *Experimental Mechanics* 46 (1) (2006) 31-38.
- [17] M. J. McGinnis, S. Pessiki, H. Turker, Application of three-dimensional digital image correlation to the core-drilling method, *Experimental Mechanics* 45 (4) (2005) 359-367.
- [18] J. Zhu, H. Xie, Z. Hu, P. Chen, Q. Zhang, Residual stress in thermal spray coatings measured by curvature based on 3D digital image correlation technique, *Surface and Coatings Technology* 206 (2011) 1396-1402.
- [19] J. D. Lord, D. Penn, P. Whitehead, The application of digital image correlation for measuring residual stress by incremental hole drilling, *Applied Mechanics and Materials* 13-14 (2008) 65-73.
- [20] A. Baldi, F. Bertolino, A low-cost residual stress measuring instrument, *Residual Stress, Thermomechanics & Infrared Imaging, Hybrid Techniques and Inverse Problems* 9 (2017) 113-119.
- [21] T. Rief, J. Hausmann, N. Motsch, Development of a New Method for Residual Stress Analysis on Fiber Reinforced Plastics with Use of Digital Image Correlation, *Key Engineering Materials* 742 (2017).
- [22] M. Hagara et al., Analysis of the aspects of residual stresses quantification performed by 3D DIC combined with standardized hole-drilling method, *Measurement* 137 (2019) 238-256.
- [23] R. Huňady, M. Hagara, M. Schrötter, Impact assessment of calibration parameters on accuracy method of digital image correlation, *Acta Mechanica Slovaca* 16(2) (2012) 6-12.